Determination of alloy interatomic potentials from liquid-state diffraction data

M. I. Mendelev and D. J. Srolovitz*
Princeton Materials Institute and Department of Mechanical & Aerospace Engineering, Princeton University, Princeton, New Jersey 08544

(Received 26 February 2002; published 16 July 2002)

This paper presents a general method for fitting interatomic potentials to partial pair correlation functions that can be obtained from diffraction experiments on pure materials or alloys. We apply this new approach to the specific case of embedded atom method-type interatomic potentials and demonstrate that it can be used to accurately fit this potential from partial pair correlation function data. The new method, presented above, can easily be extended to any type of interatomic potential. In addition, this method can be used in conjunction with standard approaches that fit crystal structure and properties.

DOI: 10.1103/PhysRevB.66.014205 PACS number(s): 61.20.Gy, 61.20.Ja, 34.20.Cf

I. INTRODUCTION

Atomistic computer simulations are widely used to investigate a broad range of material properties. While atomic interactions can be described using both quantum mechanical[1] and empirical descriptions of atomic interactions, most large scale simulations are still performed using empirical descriptions of these interactions. Empirical potentials are commonly determined by fitting a proposed functional form to available data.[2] These data may be obtained either from experimental measurements or first-principle calculations. Commonly, the input data include such quantities for crystals as lattice parameter, cohesive energy, elastic constants, and vacancy formation energy. Potentials determined in this way have found widespread use for both simulating crystals and liquids. Fitting potentials to data obtained only from perfect crystals has the disadvantage that the resultant fits are only guaranteed to be accurate at those discrete sets of interatomic spacings that are represented by the perfect crystal. This is a potential problem for applications that focus on crystal defects, competing crystal structures, and liquids. Another approach is to fit the potentials to data obtained from diffraction experiments on noncrystalline materials, which reflects a continuous distribution of atomic separations above some minimum.

The problem of determining pair potentials from the pair correlation function from single-component liquids was proposed in the framework of the classical theory of liquids more than half a century ago. While this approach was successful for low density fluids, it is less satisfactory for describing dense liquids. Fortunately, several predictor-corrector algorithms have been proposed that can be employed to find pair potentials that lead to good agreement between pair correlation functions obtained using molecular dynamics (MD) simulations and those measured experimentally.[3–6] In such algorithms, a trial pair potential is to obtain the atomic structure of the liquid (via MD simulation). Comparison of this structure and the experimental pair correlation function is used to propose a new potential that leads to improved agreement. This procedure is repeated until the discrepancy between the predicted and measured structure is within acceptable limits. These algorithms lead to a description of the atomic interactions which are consistent with the experimental diffraction data. The main disadvantage of this approach is that they are limited to pairwise descriptions of atomic interactions (i.e., pair potentials). While this is adequate for some materials (e.g., liquid argon), physically based models of interatomic interactions in many systems are intrinsically nonpairwise.

As an example, consider the case of metallic alloys, for which bonding is dominated by the electron gas contribution which cannot be described within the framework of a pair potential. A commonly used class of potentials for metallic systems is the Embedded Atom Method (EAM)[2] or Finnis–Sinclair[7] potential. In this method, the potential energy is divided into two contributions—a pairwise part and a local density part:

$$U=\sum_{i=1}^{N-1}\sum_{j=i+1}^{N}\varphi^{t_i t_j}(r_{ij})+\sum_{i=1}^{N}F(\rho_i), \tag{1}$$

where $i(j)$ labels atoms of elemental type $t_{i(j)}$, N is the number of atoms in the system, $r_{i,j}$ is the separation between atoms i and j, and

$$\rho_i=\sum_j \psi^{t_i t_j}(r_{ij}). \tag{2}$$

F, φ, and ψ are functions that must be determined. Another example is covalently bonded materials, such as Si, which are often described using three-body potentials (e.g., the Stillinger–Weber potential[8]). In both examples, the interatomic interactions are not pairwise and, hence, the above-described computer algorithms for fitting potentials to diffraction data are inapplicable. Nonetheless, there is a large body of experimentally determined diffraction data available for materials with nonpairwise interactions.

The goal of the present work is to develop a procedure for fitting arbitrary classes of interatomic potential using diffraction data from liquids (partial pair correlation functions, PPCFs). We first describe a procedure to determine interatomic potentials using atomic coordinates from a liquid. Then, we apply this approach to determine a set of EAM potentials for an alloy using partial pair correlation functions. We show that it is possible to reproduce the partial pair correlation functions using only pairwise potentials. Therefore,

this liquid structure data must be supplemented with additional information in order to completely determine the full EAM potentials. Since the goal of this paper is to show that diffraction data can be used to fit EAM potentials, we assume that the embedding part of the EAM potential is determined from other means and we simply fit the pairwise part of the EAM potential. While this particular procedure is not unique, it does demonstrate that liquid phase structural data can be used to fit nontrivial interatomic potentials. The generality of this approach is discussed at the end of this paper.

II. THEORETICAL BACKGROUND

In the method described in the following, we make use of the concept of a ''mean force,'' originally suggested in Ref. 9 for the analysis of the classical Born–Green–Bogoliubov (BGB) equation.[10,11] While the analytical solution of the BGB equation requires some simplifying approximations (e.g., superposition approximation), the concept of the mean force is general. As will be shown in the following, the mean force follows directly from Gibbs statistics and is independent of the form of the description of the atomic interactions.

We start by considering a single-component system consisting of N particles with potential energy $U(\mathbf{r}_1,\ldots,\mathbf{r}_N)$, where $\mathbf{r}_1,\mathbf{r}_2,\ldots,\mathbf{r}_N$ represent the positions of atoms 1,2,...,N. The N-particle correlation function for this system is

$$F_N(\mathbf{r}_1,\ldots,\mathbf{r}_N)=\frac{V^N}{Q_N}e^{-U(\mathbf{r}_1,\ldots,\mathbf{r}_N)/kT}, \tag{3}$$

where k is the Boltzmann constant, T is the temperature, and Q_N is the configuration integral

$$Q_N=\int e^{-U(\mathbf{r}_1,\ldots,\mathbf{r}_N)/kT}d\mathbf{r}_1\cdots d\mathbf{r}_N. \tag{4}$$

The two-particle correlation function can be obtained from the N-particle correlation function by integrating over the coordinates of all particles except particles 1 and 2:

$$F_2(\mathbf{r}_1,\mathbf{r}_2)=\frac{V^2}{Q_N}\int e^{-U(\mathbf{r}_1,\ldots,\mathbf{r}_N)/kT}d\mathbf{r}_3\cdots d\mathbf{r}_N. \tag{5}$$

We now apply the same approach used in the derivation of the BGB equation:[10] namely, we differentiate both sides of Eq. (5) with respect to the coordinates of particle 1 and substitute the expression for the N-particle correlation function [Eq. (3)]. This yields

$$kT\nabla_1\ln[F_2(\mathbf{r}_1,\mathbf{r}_2)]=-\frac{1}{V^{N-2}}\int\nabla_1U(\mathbf{r}_1,\ldots,\mathbf{r}_N)\times\frac{F_N(\mathbf{r}_1,\ldots,\mathbf{r}_N)}{F_2(\mathbf{r}_1,\mathbf{r}_2)}d\mathbf{r}_3\cdots d\mathbf{r}_N. \tag{6}$$

In a homogeneous system, the two-particle correlation function reduces to the pair correlation function: $F_2(\mathbf{r}_1,\mathbf{r}_2)=g(|\mathbf{r}_1-\mathbf{r}_2|)=g(|\mathbf{r}|)=g(r)$. Multiplying both sides of Eq. (6) by $\mathbf{r}/r$ yields:

$$kT\frac{d\ln[g(r)]}{dr}=-\frac{1}{V^{N-2}}\int[\nabla_1U_N(\mathbf{r}_1,\ldots,\mathbf{r}_N)\hat{r}]\times\frac{F_N(\mathbf{r}_1,\ldots,\mathbf{r}_N)}{F_2(\mathbf{r}_1,\mathbf{r}_2)}d\mathbf{r}_3\cdots\mathbf{r}_N. \tag{7}$$

The left-hand side of Eq. (7) is called the ''mean force,'' which we label henceforth as Φ. The mean force can be interpreted in the following manner. If the system is a low density gas, the pair correlation function is $g(r)=\exp[-\varphi(r)/kT]$ or $\varphi(r)=-kT\ln[g(r)]$, where $\varphi(r)$ is a pairwise interaction (at low densities, higher order interactions do not occur). In this case, the mean force is simply $\Phi(r)=-d\varphi/dr$. In a liquid or high density fluid, correlations beyond pair are present and therefore, the true pairwise interaction must be replaced with an effective pairwise interaction $Y(r)$, which includes the effects of all higher order interactions. In this case, the mean force is $\Phi(r)=-dY(r)/dr=kT\,d\ln[g(r)]/dr$, which is the left-hand side of Eq. (7). Equation (7) shows that the mean force is the projection of the total force $\mathbf{P}_1$ acting on atom 1 along the vector from atom 2 to atom 1, averaged over all atoms which have at least one neighbor at distance r,

$$\Phi(r)=kT\frac{d\ln[g(r)]}{dr}=\frac{1}{2}\langle(\mathbf{P}_i-\mathbf{P}_j)\delta_{r_{ij}r}\hat{r}_{ij}\rangle_{i,j}. \tag{8}$$

where δ is the Kronecker delta, $\hat{r}_{ij}$ is the unit vector pointing from atom j to i, and the average is over all pairs of atoms i,j. This equation can be extended to the case of a multicomponent system:

$$\Phi^{\alpha\beta}(r)=kT\frac{d\ln[g^{\alpha\beta}(r)]}{dr}, \tag{9a}$$

$$\Phi^{\alpha\beta}(r)=\tfrac{1}{2}\langle(\mathbf{P}_i-\mathbf{P}_j)\delta_{r_{ij}r}\delta_{\alpha t_i}\delta_{\beta t_j}\hat{r}_{ij}\rangle_{i,j}. \tag{9b}$$

No approximations were involved in deriving Eq. (9) and it is equally valid for all systems, regardless of the types of atomic interactions that are present.

Given any parametric form of an interatomic potential (EAM, three-body, four-body, etc.), we can determine $\mathbf{P}$ for the set of all atomic positions as a function of the parameters in the potential. Equation (9) shows how $\mathbf{P}$ is related to the partial pair correlation functions. The goal is to determine the values of the parameters in the potential, such that the $g^{\alpha\beta}(r)$ calculated with Eq. (9) agrees with the experimentally determined $g^{\alpha\beta}(r)$. This is now an optimization problem over the parameters in the potential. As with most nontrivial optimization problems, this procedure does not ensure that the set of parameters found is unique. In Sec. III, we apply this method to the special case of EAM potentials.

III. SELF-CONSISTENCY CHECK

In this section, we investigate the accuracy of the proposed method for fitting interatomic potentials in the following way: (1) choose an interatomic potential, (2) perform a MD simulation of the liquid and find the resultant atomic coordinates, (3) apply the above-described procedure [Eq.

TABLE I. List of all of the models and their properties.

Model[a]	Source of interatomic potential[b]	R_g	U (eV/atom)	P (GPa)	D_1 (Au) (10^5 cm^2/s)	D_2 (Cu) (10^5 cm^2/s)
M0	Ref. 12	0.000	−3.414	−0.02	2.8	3.6
P0	LJ[c]	0.220	−0.203	4.42	0.8	1.1
P1	P0	0.045	−1.145	−0.23	2.4	3.1
P2	P1	0.040	−0.942	0.77	2.4	3.6
P3	P2	0.015	−0.966	0.19	2.6	3.4
P4	P3	0.014	−0.958	0.20	2.6	3.4
P5	P4	0.015	−0.955	0.20	2.7	3.5
M1	P5	0.016	−3.446	−0.34	2.9	3.8
M2	M1	0.003	−3.406	0.16	2.8	3.8
M3	M2	0.003	−3.407	0.03	2.8	3.7
M4	M3	0.002	−3.406	0.06	2.8	3.6
N1	N0[d]	0.006	−3.421	−0.08	2.9	3.8

[a]A model consists of a set of liquid atomic coordinates and the potentials used to generate them. Model M0 is the target model (generated from the target interatomic potential from Ref. 12). Models P0–P5 were produced using only pair potentials, and models M1–M4 and N1 were determined using EAM potentials, as described in the text.

[b]The source of the interatomic potential used in the MD simulations to generate the current set of interatomic coordinates. For example, P3 in this column indicates that the interatomic potentials used to generate the atomic coordinates of model P4 were determined using the coordinates from model P3.

[c]Initial Lennard-Jones potential [Eq. (18)].

[d]EAM potentials were calculated in the same way as for series M1–M4 but with different set of basis functions.

(9)] to fit a new interatomic potential of the same general form as that used to perform the MD simulations, and (4) compare the resultant potential with the original potential. This approach allows us to reconstruct the original potential given only the atomic coordinates of the liquid generated from the original potential.

We begin by choosing a set of interatomic potentials from the class of potentials routinely used for metals, known as EAM-type potentials. The EAM potentials were designed to represent Au–Cu (crystalline) alloys.[12] These potentials are of the following functional form:

$$\varphi^{\alpha\beta}(r)=\sum_{k=1}^{k^{\alpha\beta}} a_k^{\alpha\beta}(r_{1k}^{\alpha\beta}-r)^3 H(r_{1k}^{\alpha\beta}-r), \tag{10}$$

$$\psi^{\alpha\beta}(r)=\sum_{k=1}^{k^{\alpha\beta}} b_k^{\alpha\beta}(r_{2k}^{\alpha\beta}-r)^3 H(r_{2k}^{\alpha\beta}-r), \tag{11}$$

$$F(\rho)=-\sqrt{\rho}, \tag{12}$$

where $H(x)$ is the Heaviside function, $k^{\alpha\beta}$ is the number of basis functions, α and β represent the individual elements (we arbitrarily assign $\alpha(\beta)=1$ to represent Au and 2 for Cu) and $a_k^{\alpha\beta}$, $b_k^{\alpha\beta}$, $r_{1k}^{\alpha\beta}$, and $r_{2k}^{\alpha\beta}$ are the potential parameters. The values of the potential parameters are given in the original paper.[12] While we have not investigated the degree to which this potential yields realistic results for Au–Cu alloys, this is unnecessary for our purposes here. Using this set of interatomic potentials, we performed a constant volume, constant temperature (NVT) MD simulation with 1000 Au and 1000 Cu atoms at $T=1400$ K with the density chosen such that the average pressure in the system was close to zero. The partial pair correlation functions were calculated from the resultant atomic coordinates with a histogram step size of $\Delta r=0.005$ nm. Several of the liquid state properties obtained from this model, averaged over 150 000 MD steps, are shown in Table I. In order to compare this case with others to follow, we label this model as M0.

As a first test, we compare the results of calculating the mean force $\Phi^{\alpha\beta}(r)$ directly from the PPCF of model M0 [Eq. (9a)] and by calculating $\Phi^{\alpha\beta}(r)$ from the total force **P** [Eq. (9b)]. The latter calculation [Eq. (9b)] was performed as follows. We identify all of the atomic pairs i and j of type $\alpha\beta$ that contribute to a particular bin in the PPCF histogram [$m=\text{round}(r/\Delta r)$]. Calculate the total force on atom i from all of the atoms in the system, project this force along the direction from atom j to atom i, and average this force over all such pairs of atoms separated by a distance $\Delta r(m-1/2) \leqslant r \leqslant \Delta r(m+1/2)$. The forces on the atoms were all determined using the same EAM potentials as used in the MD simulation (for M0). The result is shown as the open squares in Fig. 1, where the data were averaged over 400 independent MD configurations. Since we have replaced the true continuous PPCF with a discrete histogram of finite Δr, this calculation of the mean force is an approximation that can be improved by choosing smaller Δr (which also requires aver-

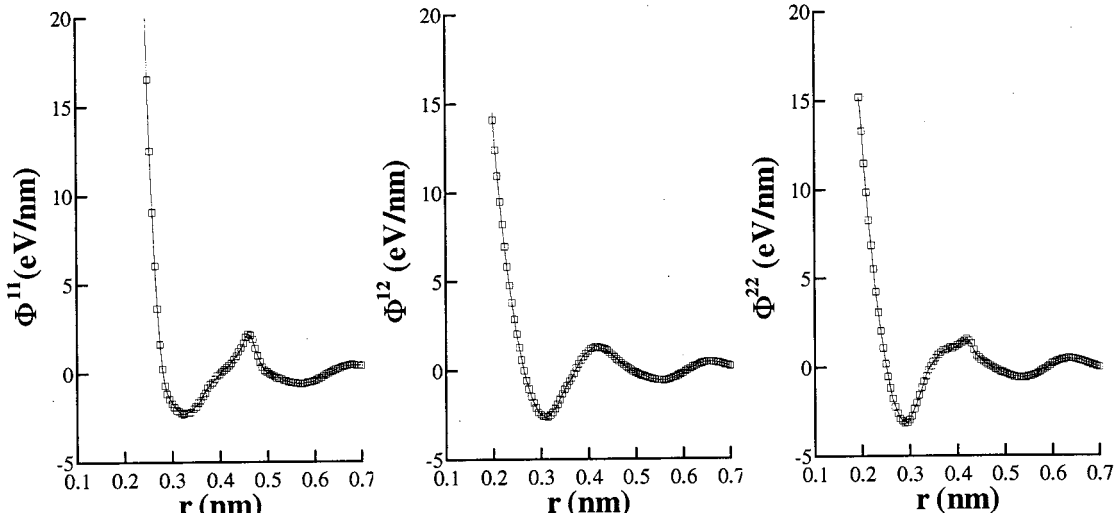

FIG. 1. Partial mean forces as a function of distance. The solid lines were determined from Eq. (9a) and the squares were determined from Eq. (9b) based on the data from model M0.

aging over many more system configurations). Examination of Fig. 1 shows that there is excellent agreement between the two approaches to calculate Φ [Eqs. (9a) and (9b)] and that the simulation conditions provide sufficient accuracy for its determination (2000 atoms, 400 independent MD configurations, $\Delta r = 5$ pm). Therefore Eq. (9) can be used to determine the parameters in interatomic potentials, as described presently.

We have demonstrated that if a specific potential yields a specific set of PPCFs, then the potential and PPCFs together must satisfy Eq. (9). We now investigate whether this is sufficient to actually determine the parameters of an interatomic potential, given a set of PPCFs. In particular, we apply this approach to determine some of the parameters in a set of alloy EAM potentials. To keep the analysis presented here simple, we focus on the parameters within the pairwise term in Eq. (1), keeping the embedding energy part fixed. In order to evaluate how well this procedure works, we will use atomic coordinates, obtained with a particular set of alloy EAM potentials (and MD), then throw out the potential and see how well we can reproduce the original potential only using the atomic coordinates. In Sec. IV, we will discuss how to do this if we only have the PPCFs, which is the main point of this paper.

We assume that we can describe the pairwise contribution to the EAM energy via

$$\varphi^{\alpha\beta}(r) = \sum_{k=1}^{k^{\alpha\beta}} a_k^{\alpha\beta} \varphi_k^{\alpha\beta}, \tag{13}$$

where $\varphi_k^{\alpha\beta}$ are basis functions of some specified form, with coefficients $a_k^{\alpha\beta}$ which must be determined. Using this postulated form of $\varphi(r)$, we can rewrite Eq. (9) as

$$\begin{aligned} kT \frac{d \ln[g^{\alpha\beta}(r_m)]}{dr} = {} & \frac{1}{4 n_m^{\alpha\beta}} \sum_{i=1}^{N} \sum_{\substack{j=1 \\ j \neq i}}^{N} \delta_{\alpha t_i} \delta_{\beta t_j} \delta_{m m_{ij}} (\mathbf{P}_i^e - \mathbf{P}_j^e) \hat{r}_{ij} \\ & - \frac{1}{4 n_m^{\alpha\beta}} \sum_{i=1}^{N} \sum_{\substack{j=1 \\ j \neq i}}^{N} \delta_{\alpha t_i} \delta_{\beta t_j} \delta_{m m_{ij}} \hat{r}_{ij} \\ & \times \left\{ \sum_{\substack{l=1 \\ l \neq i}}^{N} \sum_{k=1}^{k^{\alpha t_l}} a_k^{\alpha t_l} \frac{d \varphi_k^{\alpha t_l}(r_{il})}{dr} \hat{r}_{il} \right. \\ & \left. - \sum_{\substack{l=1 \\ l \neq j}}^{N} \sum_{k=1}^{k^{\beta t_l}} a_k^{\beta t_l} \frac{d \varphi_k^{\beta t_l}(r_{jl})}{dr} \hat{r}_{jl} \right\}, \end{aligned} \tag{14}$$

where $n_m^{\alpha\beta}$ is the number of pairs of atoms of types α and β the distance between which lies in the PPCF histogram bin with $r_m = m \Delta r$, $m_{ij} = \text{round}(r_{ij}/\Delta r)$, and $\mathbf{P}_i^e$ is the part of the total force acting on atom i associated with the embedding functions of the EAM potentials. Changing the order of summation, we can rewrite this equation in the following form:

$$\begin{aligned} & \sum_{\gamma=1}^{n_k} \sum_{k=1}^{k^{\alpha\gamma}} a_k^{\alpha\gamma} \sum_{i=1}^{N} \sum_{\substack{j=1, \\ j \neq i}}^{N} \delta_{\alpha t_i} \delta_{\beta t_j} \delta_{m m_{ij}} \hat{r}_{ij} \\ & \quad \times \sum_{\substack{l=1 \\ l \neq i}}^{N} \delta_{\gamma t_l} \frac{d \varphi_k^{\alpha t_l}(r_{il})}{dr} \hat{r}_{il} - \sum_{\gamma=1}^{n_k} \sum_{k=1}^{k^{\beta\gamma}} a_k^{\beta\gamma} \sum_{i=1}^{N} \sum_{\substack{j=1, \\ j \neq i}}^{N} \\ & \quad \times \delta_{\alpha t_i} \delta_{\beta t_j} \delta_{m m_{ij}} \hat{r}_{ij} \sum_{\substack{l=1 \\ l \neq j}}^{N} \delta_{\gamma t_l} \frac{d \varphi_k^{\beta t_l}(r_{jl})}{dr} \hat{r}_{jl} \\ & = -4 n_m^{\alpha\beta} kT \frac{d \ln[g^{\alpha\beta}(r_m)]}{dr} \\ & \quad + \sum_{i=1}^{N} \sum_{\substack{j=1, \\ j \neq i}}^{N} \delta_{\alpha t_i} \delta_{\beta t_j} \delta_{m m_{ij}} (\mathbf{P}_i^e - \mathbf{P}_j^e) \hat{r}_{ij}, \end{aligned} \tag{15}$$

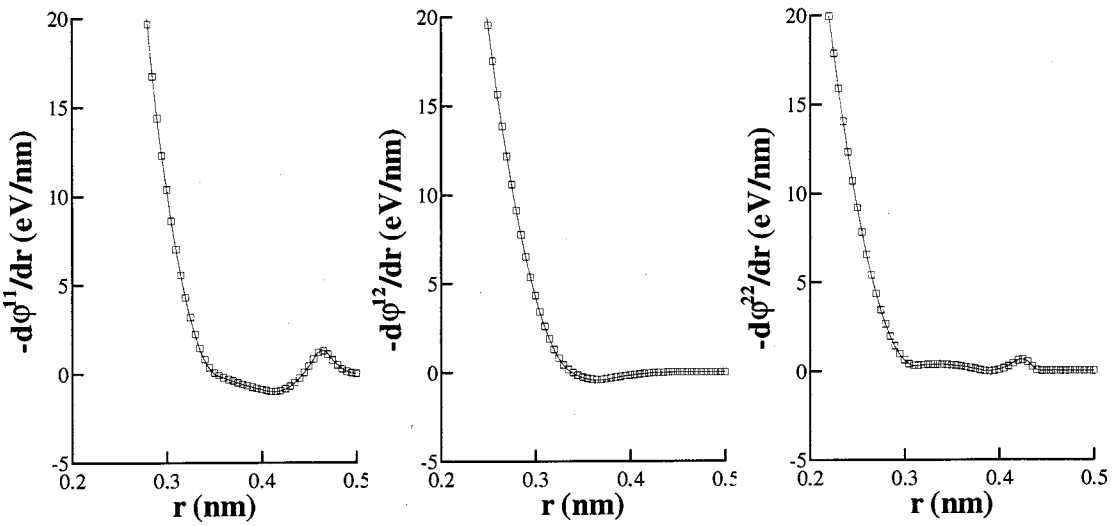

FIG. 2. Partial pair force functions vs atomic separation. The solid lines represent the original force functions (Ref. 12) and the squares represent the force functions calculated from model M0 using Eq. (15).

where n_k is the number of alloy components.

The derivatives, $d\ln[g^{\alpha\beta}(r)]/dr$, can be reliably determined only if $g > g_{\min}$, where $g_{\min}$ is determined by the accuracy to which the PPCFs are known. In the present work, the error in our calculation of the averaged PPCFs was less than 0.005 and we used a value of $g_{\min}$ which is twenty times larger ($g_{\min}=0.1$). We define $m_{\min}^{\alpha\beta}$ to be the number of the first bin in the histogram $g^{\alpha\beta}(r)$ for which $g^{\alpha\beta} > g_{\min}$ and $m_{\max}$ to be the number of the last bin for which we determined the mean force. Using this notation, Eq. (15) yields

$$\sum_{\alpha=1}^{n_k} \sum_{\beta=\alpha}^{n_k} (m_{\max} - m_{\min}^{\alpha\beta})$$

linear equations to obtain the

$$\sum_{\alpha=1}^{n_k} \sum_{\beta=\alpha}^{n_k} k^{\alpha\beta}$$

unknown coefficients $a_k^{\alpha\beta}$. We solve this system using the least-squares method. Once the $a_k^{\alpha\beta}$ are determined, the pairwise parts of the EAM potentials are known.

The results of the application of the above-described schema to the original set of atomic coordinates obtained from MD simulations using the EAM potentials of Ref. 12 are shown in Fig. 2. The choice of basis functions in Eq. (13) is arbitrary, however, in the present case, we assume the same form of basis functions as used in the original set of EAM potentials [Eq. (10), i.e., $\varphi_k^{\alpha\beta} = (r_{1k}^{\alpha\beta} - r)^3 H(r_{1k}^{\alpha\beta} - r)$]. Figure 2 shows that we can exactly reconstruct the pairwise parts of the EAM potentials given the atomic coordinates and the embedding energy parts of the EAM potentials.

While the application of the method described here was to determine only the pairwise parts of the potential, the method relating the potential to the total force is general and could be applied to all of the functions in an EAM potential. However, in this case, the resultant equations are not linear and, hence, more care must be exercised to avoid problems associated with multiple minima and more computer time will be required.

IV. CALCULATION OF THE PAIRWISE PART OF EAM POTENTIALS FROM PPCFs

In Sec. III, we fit the potential using a full set of liquid state atomic coordinates. However, the coordinates of all of the atoms in a liquid cannot be obtained experimentally. Rather, diffraction experiments only yield total pair correlation functions. If the number of independent diffraction experiments is greater or equal to $n_k(n_k+1)/2$ we can extract the partial pair correlation functions. In the present work, we focus on two-component alloys for which all three PPCFs are known.

To use the above-described schema we must first obtain the atomic coordinates. However, these are not available from MD since the interatomic potentials are unknown. Thus we shall use a predictor-corrector procedure which will allow us to simultaneously obtain a set of atomic coordinates and EAM potentials consistent with the PPCFs. Such a procedure for strictly pairwise potentials was described in Ref. 5. This procedures starts from an initial guess for the atomic coordinates. We then use Eq. (15) with the target (e.g., those from diffraction experiments) PPCFs and this set of atomic coordinates to obtain a set of EAM potentials. These EAM potentials are then used in a MD simulation of the liquid to obtain a new set of atomic coordinates. This new set of atomic coordinates and the target PPCFs are then used to find a new set of EAM potentials using Eq. (15). This procedure is repeated until further iterations no longer improve the agreement between the PPCFs obtained from the MD simulations and the target PPCFs. As a quantitative measure of the discrepancy between the model and target PPCFs we use the rms error

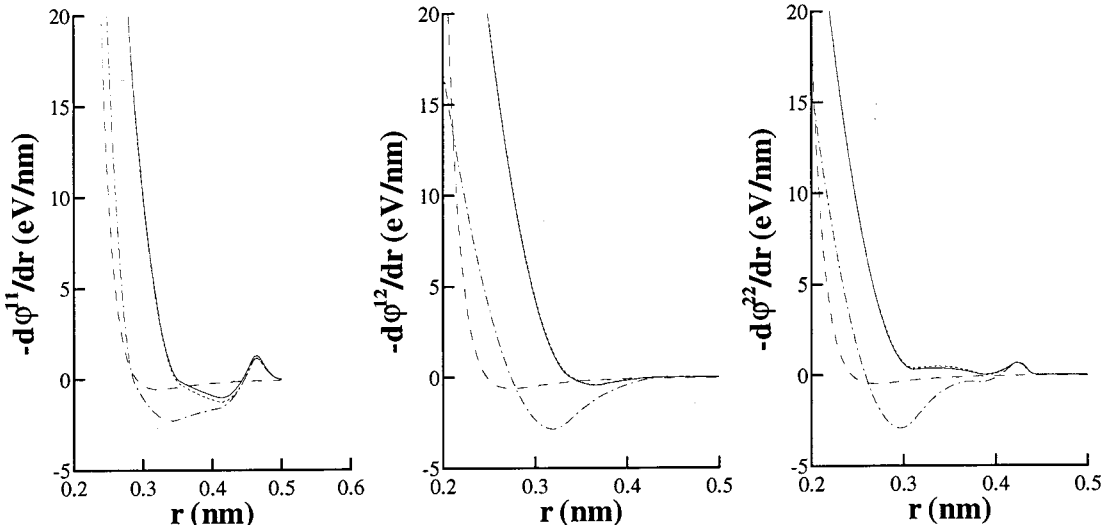

FIG. 3. Partial pair force functions vs atomic separation. The solid lines represent the original force functions (Ref. 12), the dashed lines represent the initial Lennard-Jones force functions used to create model P0. The dash-dot lines are the force functions associated with interatomic potentials that are purely pairwise and were derived from model P4. The dotted lines are the force functions derived associated with interatomic potentials that include both pairwise and embedding energy terms and were derived from model P5 (which itself was created only using pairwise potentials). The force functions associated with M4 are plotted, but are indistinguishable from the original force functions (solid lines).

$$R_g = \left\{ \frac{2}{n_k(n_k+1)m_{\max}} \sum_{\alpha=1}^{n_k} \sum_{\beta=\alpha}^{n_k} \sum_{m=1}^{m_{\max}} (g^{\alpha\beta}(r_m) - g_0^{\alpha\beta}(r_m))^2 \right\}^{1/2}. \tag{16}$$

We can augment the total force equation [Eq. (15)] employed to fit the potentials by also making use of the condition that average pressure in the system is fixed at atmospheric pressure, which is approximately zero. If we assume that the pairwise part of the EAM potentials is described by Eq. (13), this condition yields an additional equation which is linear in the unknown coefficients $a_k^{\alpha\beta}$:

$$\sum_{\alpha=1}^{n_k} \sum_{\beta=\alpha}^{n_k} \sum_{k=1}^{k^{\alpha\beta}} a_k^{\alpha\beta} \sum_{i=1}^{N} \sum_{j=i+1}^{N} \delta_{\alpha t_i} \delta_{\beta t_j} r_{ij} \frac{d\varphi_k^{\alpha\beta}(r_{ij})}{dr} = -3NkT - 3Vp^e, \tag{17}$$

where p^e is the contribution to the pressure from the embedding energy. To solve Eqs. (15) and (17) simultaneously, we multiplied Eq. (15) by $(1-\alpha)$ and Eq. (17) by α. If $\alpha=0$, we fully neglect the pressure condition, Eq. (17). We vary α in the range $0.02 \leqslant \alpha \leqslant 0.05$, when we expressed the force in eV/Å and the pressure in GPa.

We begin the potential fitting procedure by creating a set of atomic coordinates using a crude pairwise potential, i.e., the Lennard-Jones potentials

$$\varphi^{\alpha\beta}(r) = \varepsilon^{\alpha\beta}\left[\left(\frac{r_0^{\alpha\beta}}{r}\right)^{12} - 2\left(\frac{r_0^{\alpha\beta}}{r}\right)^{6}\right], \tag{18}$$

the parameters $\varepsilon^{\alpha\beta}$ and $r_0^{\alpha\beta}$ of which were obtained by a least-squares fit of $-kT\ln[g^{\alpha\beta}(r)] = \varphi^{\alpha\beta}(r)$. The dependence of the interatomic force with atomic separation [i.e., $-d\varphi^{\alpha\beta}(r)/dr$] obtained from these pair potentials are shown in Fig. 3. Molecular dynamics simulations performed with this potential give the initial set of atomic coordinates, which we label as model P0. Figure 4 shows a comparison between the PPCFs of model P0 and the target PPCFs. The agreement between the two is very poor, as expected given the nature of the initial description of the atomic interactions (i.e., Lennard-Jones). Nonetheless, we can use the atomic coordinates from model P0 to obtain an improved potential.

In order to make the computation as efficient as possible, it is advantageous to use the best initial structure we can obtain before using the full potential (i.e., pairwise plus embedding terms). To this end, we first optimize the atomic structure using just a pair potential, i.e., we assume that the embedding energy is exactly zero for now. Of course, we do not expect that this approach will yield a potential that is able to fully describe the experimental PPCFs, but rather it will provide a better starting structure for use in fitting the real EAM potential (i.e., with a real embedding term).

Table I shows the results of the iterations (the P1–P5 series) between the pair potentials and atomic models to obtain improved agreement between the model and target PPCFs. In particular, Table I shows the rms error between the model and target PPCFs, R_g. Clearly, the agreement between the two initially improves rapidly with iteration until further iteration no longer improves R_g. These results suggest that it is not possible to achieve excellent agreement between the model and target PPCFs without including the embedding energy (i.e., only including the pairwise terms). It should be noted, however, that the remaining discrepancy ($\sim$0.015) is

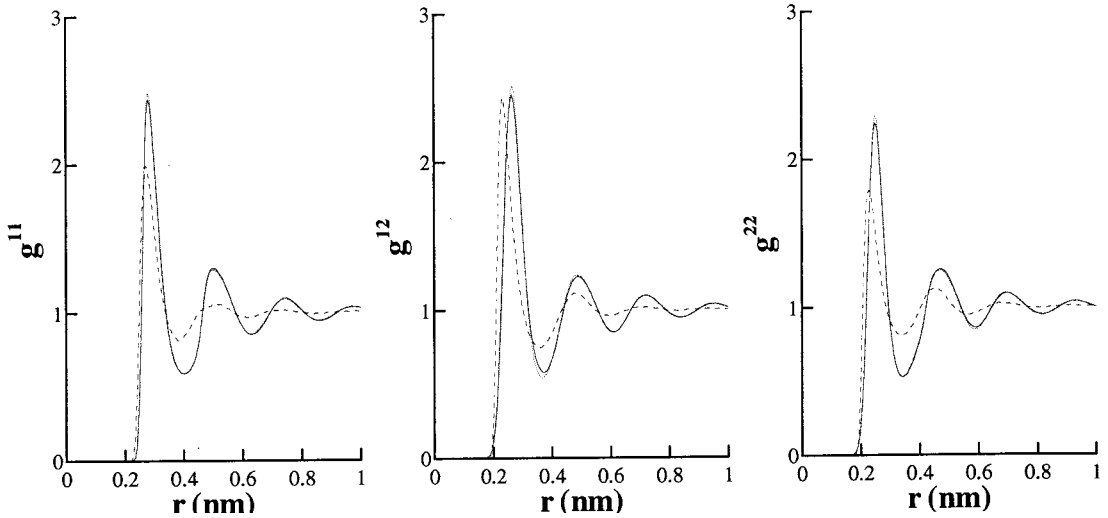

FIG. 4. Partial pair correlation functions vs interatomic separations. The line types are the same as in Fig. 3.

already smaller than current experimental error in determining the PPCFs for liquid metallic alloys. The pair potentials obtained to this point were based on the assumption that the system can be described on the basis of pairwise interaction alone. Therefore, it is not surprising that the resultant pair potentials are quite different from the pairwise part of the original EAM potentials, as shown in Fig. 3.

Now we return to the main focus of the present investigation—that is, the question of whether we can reconstruct the pairwise part of the EAM potentials from the target PPCFs. (We assume that the embedding energy contribution to the potential is known.) To this end, we reconstruct the pairwise part of the EAM potentials based upon the final set of atomic coordinates obtained from the pair potentials, i.e., model P5 and the target PPCFs [i.e., where now the P^e and p^e terms in Eqs. (15) and (17), respectively, are included]. Figure 3 shows that the pair forces, obtained in this way, are nearly indistinguishable from the original ones. We performed molecular dynamics simulations using these new pairwise potentials and the original embedding energy part to obtain the atomic coordinates of model M1. The above-described iterative procedure is applied until the rms error between the model and target PPCFs no longer improves. The results of this iterative procedure are shown in Table I as M1–M4. The errors initially decrease rapidly and then saturate at $R_g = 0.002$. The resultant and target PPCFs are completely indistinguishable (see Fig. 4), as are the resultant and original pairwise pars of the EAM potential (Fig. 3).

In addition to examining the discrepancies between the model and target PPCFs, we monitored two properties of the system—the potential energy and the diffusivities of the two alloy components. While the agreement between the potential energies of the model described purely on the basis of pair potentials and the original model is poor, the potential energy obtained from model M4 (i.e., the fitted EAM potential) agrees very well with the original value (i.e., to within 0.23%). The diffusivity data in Table I demonstrate that the diffusivities are equally well reproduced by models P5 and M4. This shows that while the embedding term is necessary for quantitatively describing thermodynamic properties, some kinetic properties can be well described purely on the basis of pairwise interactions.

In the above-examined examples, we chose to use the same set of basis functions as in the original EAM potentials (which was used to create the model M0), i.e., $\varphi_k^{\alpha\beta} = (r_{1k}^{\alpha\beta} - r)^3 H(r_{1k}^{\alpha\beta} - r)$. In most real cases where we are trying to fit potentials, we do not have the luxury of knowing *a priori* the appropriate form of the basis functions. In fact, we will, in general, simply have to assume a particular set of basis functions and use the above-described procedure to simply determine the coefficients of each. This same issue arises in all potential fitting activities. In order to determine the sensitivity of our results to the form of the basis functions employed, we repeated the whole procedure where we use $\varphi_k^{\alpha\beta} = (r_{1k}^{\alpha\beta} - r)^p H(r_{1k}^{\alpha\beta} - r)$ and $p = 4$ or 5. In particular, we used 10 basis functions and the same $r_{1k}^{\alpha\beta}$ (uniformly distributed between 0.32 and 0.50 nm) for all three pair potentials. The result of refitting the potentials from the PPCFs using these new basis functions is shown in Fig. 5. Clearly, the agreement is excellent, but not perfect. Therefore, the results are not very sensitive to the exact nature of the basis functions used to fit the potentials. Some of the discrepancy between the original pairwise potentials and the refit potentials (using the new basis functions) comes from the fact that it is not possible to exactly reproduce one curve by fitting a set of functions of different form to it. This is demonstrated in Fig. 5, where we have performed a least-squares fit of the new basis functions to the original potential. As expected, this procedure does not exactly reproduce the original functions. Therefore, we can conclude that the discrepancy between the pair potentials obtained using different basis functions is intrinsic to the choice of the functional forms of the potentials assumed. As a final check, we calculated the energy and diffusivities associated with the atomic structures obtained by refitting the EAM potentials with the new basis functions (labeled N1). Like the properties obtained from the fitting using the original basis functions, M4, the properties ob-

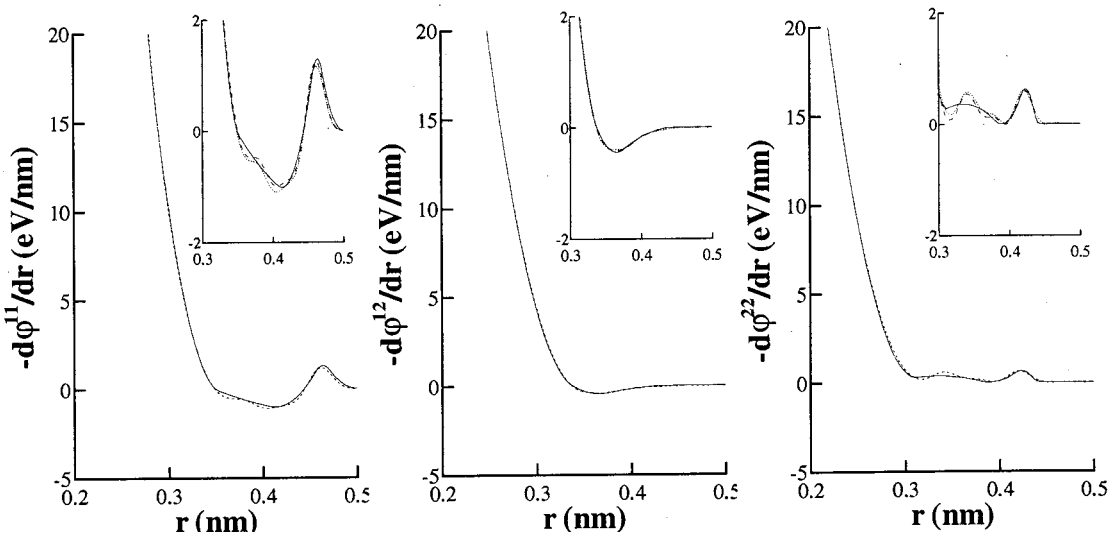

FIG. 5. Partial pair force functions vs interatomic separations. The solid lines represent the original force functions and the dotted lines represent the force function used to create model N1 (see the text). The dashed lines represent the best fitting of the original pairwise force functions by linear combination of the new basis functions used to create pairwise force functions for model N1 (see the text).

tained from fitting to the new basis functions are in excellent agreement with the original model, M0.

V. CONCLUSIONS

In this paper, we presented a general method for fitting interatomic potentials to partial pair correlation functions that can be obtained from diffraction experiments on pure materials or alloys. We applied this new approach to the specific case of embedded atom method-type interatomic potentials, which have both pairwise and embedding energy terms. To make the method more transparent, we limit consideration herein to the special case in which the embedding energy part of the potential is known. Using this approach, we have demonstrated that this method can accurately reconstruct the pairwise part of this potential from PPCF data. While the present example was limited, more commonly both the pairwise and embedding terms in the energy must be determined. The new method, presented previously, can easily be extended to fit both parts of the EAM potential. Moreover, this same procedure can be applied to any other type of interatomic potential. For example, it is a simple matter to derive equations analogous to Eqs. (15) and (17) for interatomic potentials that contain both two-body and three-body terms.

Most of the EAM-type potentials in the literature were determined by fitting the constituent functions of the EAM potentials to experimental and/or first-principles data for crystals (e.g., cohesive energy, lattice parameter, elastic constants, vacancy formation energy, surface energies). The above-suggested iteration procedure for fitting potentials can incorporate the same types of crystal data *in addition to* the liquid state data (PPCFs and density). Indeed, each crystal property available simply provides one new equation to determine the potential parameters. We can solve all of these equations simultaneously, together with Eqs. (15) and (17) for the liquid state data. In this case, however, the potentials should be able to describe both the crystalline and liquid phase structure and properties. The ability to accurately and simultaneously describe both liquids and solids can be very important, for example, for the simulation of solidification processes.

The main equation used in this new procedure for fitting potentials is derived from Gibbs statistics and, therefore, is applicable to equilibrium systems. However, in Ref. 5, it was shown that the Born–Green–Bogoliubov equation (derived from Gibbs statistics) can be used to determine pair potentials from (metastable) metallic glass PPCFs. Therefore, we expect that the procedure suggested here is also applicable to metallic glasses. This is noteworthy since considerably more diffraction data are available for glasses than for liquids.

ACKNOWLEDGMENTS

The authors gratefully acknowledge helpful and fruitful discussions with Professor Graeme J. Ackland. This research was supported by the U.S. Department of Energy through Grant No. DE-FG02-99ER45797 and its Computational Materials Science Network.

*Corresponding author; email address: srol@princeton.edu

[1] R. Car and M. Parrinello, Phys. Rev. Lett. **60**, 204 (1988).
[2] M. S. Daw and M. I. Baskes, Phys. Rev. B **29**, 6443 (1984).
[3] W. Schommers, Phys. Lett. A **43**, 157 (1973).
[4] L. Reatto, Philos. Mag. A **58**, 37 (1988).
[5] M. I. Mendelev, J. Non-Cryst. Solids **223**, 230 (1998).
[6] D. K. Belashchenko, J. Inorg. Chem. **37**, 501 (2001).
[7] M. W. Finnis and J. E. Sinclair, Phys. Lett. A **50**, 45 (1984).

[8] F. H. Stillinger and T. A. Weber, Phys. Rev. B **31**, 5262 (1985).
[9] M. D. Johnson, P. Hutchinson, and N. M. March, Proc. R. Soc. London Sect. **282**, 283 (1964).
[10] N. N. Bogoliubov, *Problems of the Dynamic Theory in Statistic Physics*, (Gostechizdat, Moscow, 1946).
[11] M. Born and H. Green, Proc. R. Soc. London, Ser. A **188**, 10 (1946).
[12] G. J. Ackland and V. Vitek, Phys. Rev. B **41**, 10324 (1989).